Positron and electron-impact multiple-ionization

2015 J. Phys. B: At. Mol. Opt. Phys. 48 165203

(http://iopscience.iop.org/0953-4075/48/16/165203)

IOP Publishing
Journal of Physics B: Atomic, Molecular and Optical Physics
J. Phys. B: At. Mol. Opt. Phys. 48 (2015) 165203 (11pp)
doi:10.1088/0953-4075/48/16/165203

Positron and electron-impact multiple-ionization

C C Montanari[1,2] **and J E Miraglia**[1,2]

[1] Instituto de Astronomía y Física del Espacio, Consejo Nacional de Investigaciones Científicas y Técnicas and Universidad de Buenos Aires, C1428EGA, Buenos Aires, Argentina
[2] Facultad de Ciencias Exactas y Naturales, Universidad de Buenos Aires, Buenos Aires, Argentina

E-mail: mclaudia@iafe.uba.ar

Received 11 February 2015, revised 17 May 2015
Accepted for publication 29 May 2015
Published 10 July 2015

Abstract

We present positron-impact multiple (single to quintuple) and total ionization cross sections of Ne, Ar, Kr, and Xe, covering an extended energy range from 50 eV to 7 keV. We improve on previous calculations of the ionization thresholds by adding the mean kinetic energy transferred to the target electrons. In this way the thresholds compare rather well with the experimental appearance energies for the different *k*-fold ionization cross sections. Present results include not only the novel energy threshold at low energies but also the post-collisional contribution at high energies. We performed a quite complete particle–antiparticle comparison by including our positron-impact results, new calculations for electron-impact ionization including the threshold correction, and a detailed compilation of experimental data. Present positron-impact multiple ionization cross sections are the first ones in such an extended energy region.

Keywords: positron, electron, multipleionization

1. Introduction

Multiple ionization (MI) processes play an important role in understanding the physics of the many-electron problems, such as multiple-electron transitions, collisional and post-collisional electron emissions or electron correlation effects. In addition, the comparative study of particle–antiparticle values (electrons–positrons, protons–antiprotons) contributes to the analysis of the dominant mechanisms in the intermediate-to low-energy region where differences are clear, i.e. charge and mass effects, polarization and differences in projectile trajectories. Some reviews on particle–antiparticle collisions can be found in [1–4], and particularly for positrons in [5–9]. Positron-impact ionization remains an interesting subject of experimental and theoretical study due to its applications (astrophysics, medicine, material science) [10], its experimental possibilities compared with antiproton sources (antiproton sources rely on high-energy experiments such as the antiproton decelerator facility at CERN), and more efficient ionization compared to electron impact (i.e. higher ionization cross sections in the intermediate energy region) [11].

Recently many articles have focused on the study of positron interaction with atoms [12–14] and molecules [11, 15, 16]. Most of the studies on ionization by positrons are about total or single ionization, experimentally [17–21] or theoretically [22–25]; few articles report double or triple ionization [26–33], and only one reports quadruple-ionization ([31], just for Xe). To our knowledge no theoretical proposals have been put forward to describe the positron-impact MI problem in a broad and comprehensive manner, encompassing single to quintuple-ionization, from threshold to high energies. This paper is a step in that direction.

In the last few years we have studied the MI by extensively applying different strategies. We have dealt with MI by impact of protons [34], antiprotons [35], and lately electrons [36]. In this article we close this sequence by calculating MI by impact of positrons.

Our basic consideration is the assumption of the independent particle model (IPM), i.e. that the ejected electrons ignore each others' fate, neglecting the correlation in the final state. Within the IPM, the probability of MI is expressed as a multinomial combination of independent ionization probabilities of the different subshells [37, 38]. Our calculations employ the continuum distorted-wave eikonal initial state (CDW-EIS) approximation for ionization probabilities as a function of the impact parameter [34–36, 39, 40]. We have also calculated the first Born approximation to confirm the

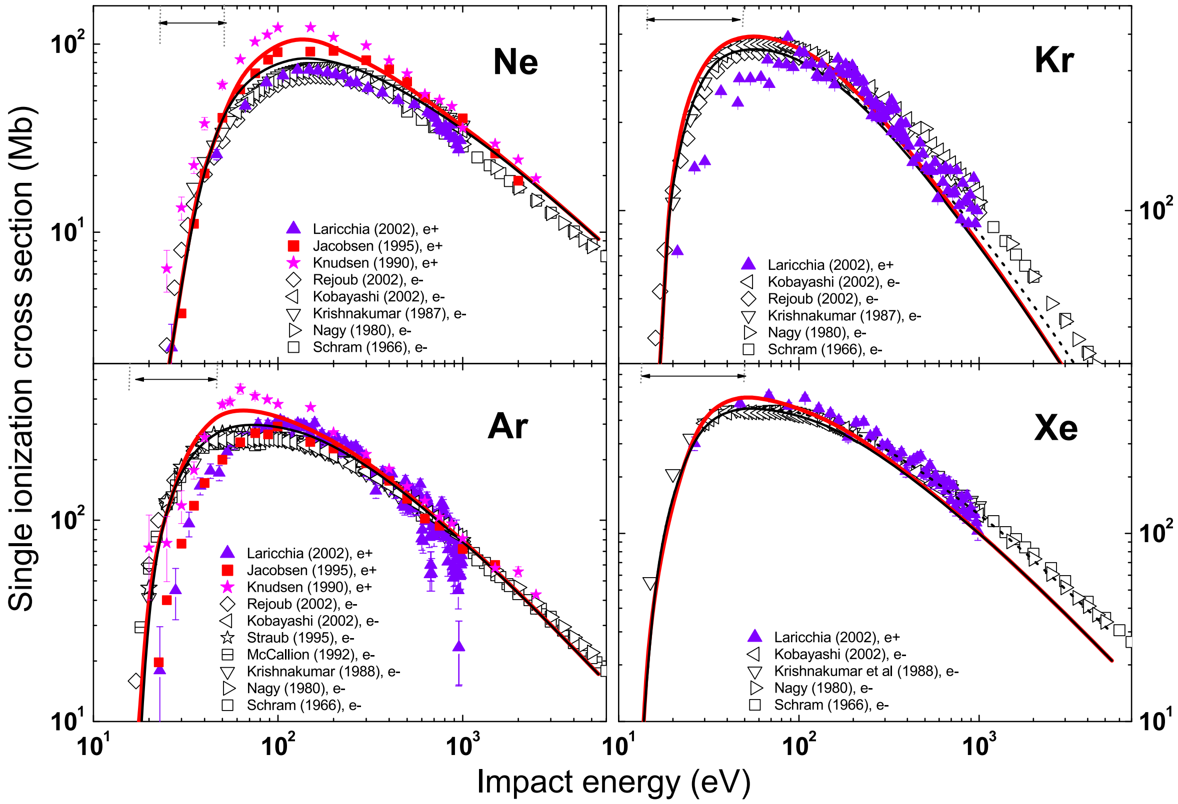

Figure 1. Single-ionization cross sections of Ne, Ar, Kr and Xe by positron and electron impact. Curves present results for positron impact (red-thick curve) and by electron-impact (black-thin curve) including direct and post-collisional ionization; dashed-curve presents results for direct ionization by electron impact. Experimental data: **for positron impact**, ▲ Laricchia *et al* [20] (renormalization of [27]), ■ Jacobsen *et al* [18], ☆ Knudsen *et al* [17]; **for electron impact**, ◊ Rejoub *et al* [62], ◁ Kobayashi *et al* [63], ⊟ McCallion *et al* [64], ▿ Krishnakumar *et al* [53], ▷ Nagy *et al* [56], □ Schram *et al* [55], hollow ★ Straub *et al* [65]. The double arrow indicates the region where the theoretical values are interpolated, from the last not-null CDW-EIS cross section, to zero for the appearance energy.

high-energy limit. As the CDW-EIS is an approximation valid for heavy projectiles, to deal with the positron and electron impact we have corrected the probabilities to account for the light mass, the momentum and energy transferred, the non-linear trajectory and the minimum energy required for MI. All these corrections have been explained in detail in [36] for the electron impact. For the positron impact we follow the same pattern. The only difference is that for positrons the trajectories are repulsive, and as a consequence there is an exclusion zone that the projectile cannot visit (see figure 1 of [36]).

Two different ionization mechanisms are responsible for the target final charge state: the direct ionization (DI) and the post-collisional ionization (PCI). The first one is the known electron emission due to the projectile interaction with the target bound electrons. It is important in the low- and intermediate-energy region but decreases drastically for high-impact energies. The second one is the electron emission cascade that follows inner-shell ionization, which determines the final ion charge state. PCI is independent from the projectile and may be incorporated using photoionization data [37, 38]. In the present contribution we follow the same method as in [34–36].

Concerning the energy threshold, in [36] we assumed that the minimum impact energy for MI was just the addition of the binding energies of the emitted electrons. By doing so we clearly underestimated the experimental appearance energies for k-fold ionization with $k \geqslant 2$ [36]. In the present contribution we have improved our previous estimation by considering not only the binding energies but also the average kinetic energy of each electron on its way out. In this manner the comparison with the experimental appearance energies is highly improved [41].

The paper is organized as follows. In section 2 we state the physical considerations regarding the threshold for MI by light particles (section 2.1) and the inclusion of PCI (section 2.2). In section 3 we comment about the positron impact experimental data and their normalizations. Finally, in section 4 we present and discuss our theoretical results for positron and electron-impact MI and total ionization cross sections of the heavier rare gases (starting with Ne). Detailed comparison with experiments is made. Atomic units are used except when it is indicated.

2. Theoretical considerations

2.1. The energy threshold

The energy threshold in MI is a key point that has deserved much theoretical and experimental effort [17, 42–46]. If we

Table 1. Ionization thresholds (in eV) for k-fold direct ionization of Ne, Ar, Kr and Xe by positron or electron-impact, in Thompson approximation, using the mean energy transferred given by equation (2).

K	1	2	3	4	5	6
Ne	23.1	81.3	155	239	331	428
Ar	16.1	56.5	108	166.4	230	298
Kr	14.2	50.1	95.7	147.5	204	264
Xe	13.0	43.7	83.5	128.8	178	230

consider k-fold ionization, the total energy transferred to the target electrons is

$$E^{(k)} = \sum_{nl} q_{nl}\ E_{nl}, \tag{1}$$

where q_{nl} is the number of electrons removed from the nl-subshell, E_{nl} is the energy transferred to each electron, and $k = \sum_{nl} q_{nl}$. Thus the threshold is given by $\overline{E}^{(k)}$ corresponding to the minimum value of E_{nl}, denoted with $\overline{E}_{nl}$. In our previous calculation we just considered $\overline{E}_{nl} = I_{nl}$, with I_{nl} being the orbital binding energy [36]. In the present contribution we have improved this value by considering not only I_{nl} *but also* the mean kinetic energy of the emitted electrons. Using the classical Thompson approximation [47] for light projectiles, it can be shown that $\overline{E}_{nl}$ should be [41]

$$\overline{E}_{nl} = \frac{E\ I_{nl}\ Ln\left(E/I_{nl}\right)}{\left(E - I_{nl}\right)}\ >\ I_{nl}. \tag{2}$$

This is an energy threshold that depends on the impact energy E. It is greater than I_{nl}, but tends to it if the impact-energy is sufficiently low,

$$\lim_{E \to I_{nl}} \overline{E}_{nl} = I_{nl}. \tag{3}$$

This threshold is not a general cut-off; we have to include $\overline{E}_{nl}$ within the multinomial expansion. For example, for the quadruple ionization of Xe we needed to consider different thresholds for each of the 467 terms [48]. The inclusion of the minimum energy given by equation (2) within the MI calculations makes a dramatic difference in the electron and positron-impact cross sections in the low-energy region.

The experimental *appearance* energies in k-fold ionization have been compiled by Denifi *et al* [42, 43]. We have estimated these values considering that all the electrons are emitted from the outermost shell (the most loosely bound electrons),

$$\overline{E}^{(k)}_{\min} \simeq \overline{E}^{(k)}_{\text{out}}\ =\ k\ \overline{E}_{nl=\text{out}}. \tag{4}$$

In table 1 we display our results for $\overline{E}^{(k)}_{\min}$ given by equation (4) for single ($k = 1$) to sextuple ($k = 6$) ionization of Ne, Ar, Kr and Xe. The comparison with the experimental values tabulated by Denifi *et al* [42, 43] is quite reasonable as shown in figure 2 of [41]. As an illustration, let us focus on the triple ionization of Ar. By considering just the binding energy $I_{3p} = 16.1$ eV, the threshold would be at $3 \times I_{3p} = 48.2$ eV, while the experimental value is 84 eV [42, 49]. Instead, using (4) $\overline{E}^{(k)}_{\min} = 108$ eV. The extra 60 eV (difference between 48.2 eV and 108 eV) is the averaged kinetic energy of the three emitted electrons. The present value is much closer to the experimental one but still overestimates due to limitations of our model, i.e. the IPM, the Thompson approximation, and even the absence of sequentiality within the MI processes, which plays an important role.

For positron-Ar ionization the threshold measured by McEachran *et al* [10] is higher than the electron-impact one. This is not predicted by our simple model, which gives the same value for both electrons and positrons. The experimental minimum energy for positron-impact ionization is not as clear as for electron impact. Low-energy positron-impact collisions may lead to positronium formation. The separation between positronium formation and pure ionization is a sensitive point in this energy region [20] and may affect the determination of the ionization threshold.

Note that the values in table 1 correspond to DI while the experimental ones include DI + PCI. From single to triple ionization PCI is almost negligible near the threshold. However, this is not true for k-fold ionization, with $k \geqslant 4$. This can produce highly charged ions for impact energies below those in table 1. We will return to this point in section 4.

2.2. The post-collisional processes

When an electron is removed from a deep shell, cascades of different processes take place (Auger-type processes, radiative decays or combination of both). Thus the final (measured) charge state is higher than the DI prediction. For example, above 1 keV the $3d$ single ionization of Xe is critical to describe the quintupleonization [48], and so are the $2p$ of Kr and $3p$ of Xe for the sextuple ionization.

We include PCI within the MI as in previous works [34–36]. The method considers the experimental branching ratios of the charge-state distribution after a single initial vacancy, and incorporates them within the multinomial expansion [37, 38]. Thus DI turns into *total* MI, including PCI. Pioneering in this research are the works by Carlson and coworkers [50, 51], used in multiple-ionization calculations too [37, 38, 52]. Due to the advances in photoionization experimental techniques, quite a lot of new research has been carried out in the last twenty years. Improved values and details of the Auger processes are available in the literature. Updated tabulations of the experimental branching ratios for PCI of Ne, Ar, Kr and Xe can be found in [36].

3. Considerations about the experimental data

Despite its technological and medical possibilities [10] the experimental data on total ionization and MI by positron-impact is much more scarce than electron-impact measurements. A key point is the normalization of the relative values. Positron experiments are usually normalized to the total ionization cross sections by electron impact assuming that at sufficiently high energies both values converge. For example, Kara *et al* [27] and Jacobsen *et al* [18] normalized to the single-ionization cross sections by Krishnakumar and

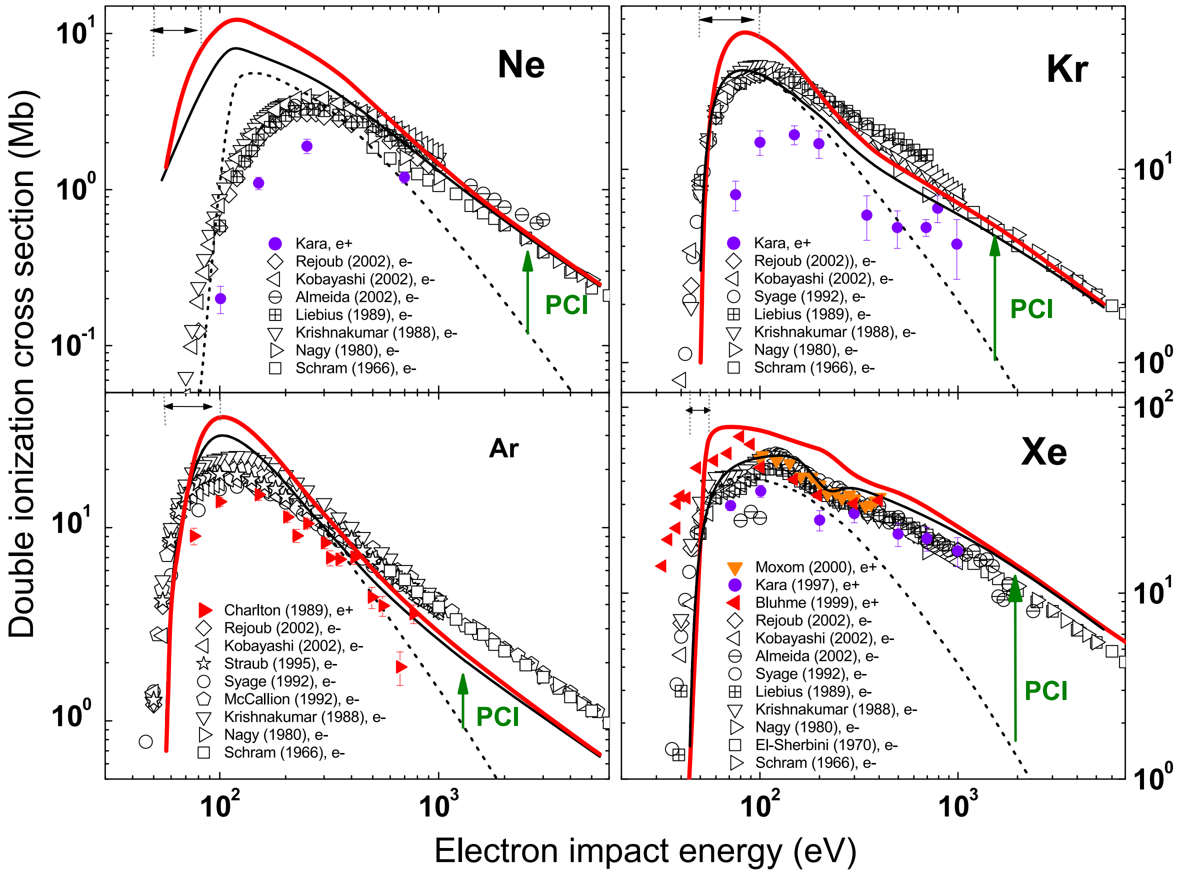

Figure 2. Double ionization cross sections of Ne, Ar, Kr and Xe by positron and electron-impact. Curves as in figure 1. Symbols: **for positron impact**, ● Kara *et al* [27], ▶ Charlton *et al* [26] (in Laricchia *et al* [6]), ▲ Moxom *et al* [31], ◀ Bluhme *et al* [30] (only for energies above 60 eV, the lower energy values include positronium formation); **for electron impact**, ∘ Syage [49], ▿ Krishnakumar *et al* [53], □ Schram *et al* [55], ▷ Nagy *et al* [56], ◊ Rejoub *et al* [62], ⊟ McCallion *et al* [64], ◁ Kobayashi *et al* [63], ⊖ Almeida *et al* [66], ⊞ Liebius *et al* [67], hollow ⋆ Straub *et al* [65]. The double arrow indicates the region where the theoretical values are interpolated, from the last not-null CDW-EIS cross section, to zero for the appearance energy.

Srivastava [53], while Knudsen *et al* [17] normalized to the total ionization cross sections by Rapp and Englander-Golden [54]. Differences should be small because Krishnakumar and Srivastava [53] values are not absolute ones and have been normalized to the total cross sections by Rapp and Englander-Golden [54]. Another possibility is the normalization with the absolute data by Schram [55], Nagy [56] or by Sorokin *et al* [57, 58] as in Laricchia *et al* [20], which produces a clear difference for total ionization cross sections of Ne.

The choice of the electron-impact total cross sections for the normalization is a point of discussion [59]. Many factors must be considered. The first one is that few electron measurements are absolute cross sections with low relative errors, as noted by Sorokin *et al* [57]. Reference values for total ionization cross sections are the measurements by Rapp and Englander-Golden [54], by Schram *et al* [55], and much more recently, by Sorokin *et al* [57, 58].

The method used by Sorokin and collaborators reduces the experimental error below 2% by comparing ionization by electrons and by photons. However it should be noted that while the *total* ionization cross sections by Rapp and Englander-Golden [54] are *gross* cross sections, $\sigma_{\text{gross}} = \Sigma\ k\ \sigma_k$, the *total* cross sections by Sorokin *et al* [57, 58] are *count* cross sections (direct addition of the different *k*-fold ionization cross sections $\sigma_{\text{count}} = \Sigma\sigma_k$). Unfortunately, both are named *total* ionization cross sections. Experimentally, *gross* is flux of emitted electrons while *count* is flux of positive ions. The total cross sections calculated as $\sigma_{\text{total}} = \Sigma\sigma_{nl}$, with *nl* being the initial bound state, are actually *gross* cross sections [60]. See [35] for a detailed discussion on this subject. We have found that the difference between gross and count cross sections is almost negligible for Ne and Ar, but it is important for Kr and Xe (at 1 keV they are 22 and 34% respectively). A possibility in order to compare *gross* and *count* cross sections is to use the tabulated ratios gross/count. Tables of these ratios can be found in [35] (theoretical values for proton and antiproton impact) and in [61] (experimental values for electron impact). Both tables show good agreement in the high-energy region where heavy and light particle values converge. Considering the count-to-gross ratios, the measurements by Sorokin *et al* [57, 58] are in good agreement with Schram [55] for Ne, Ar, Kr and Xe, and also with Rapp and Eglander-Golden [54], except in the case of Ne [57, 58].

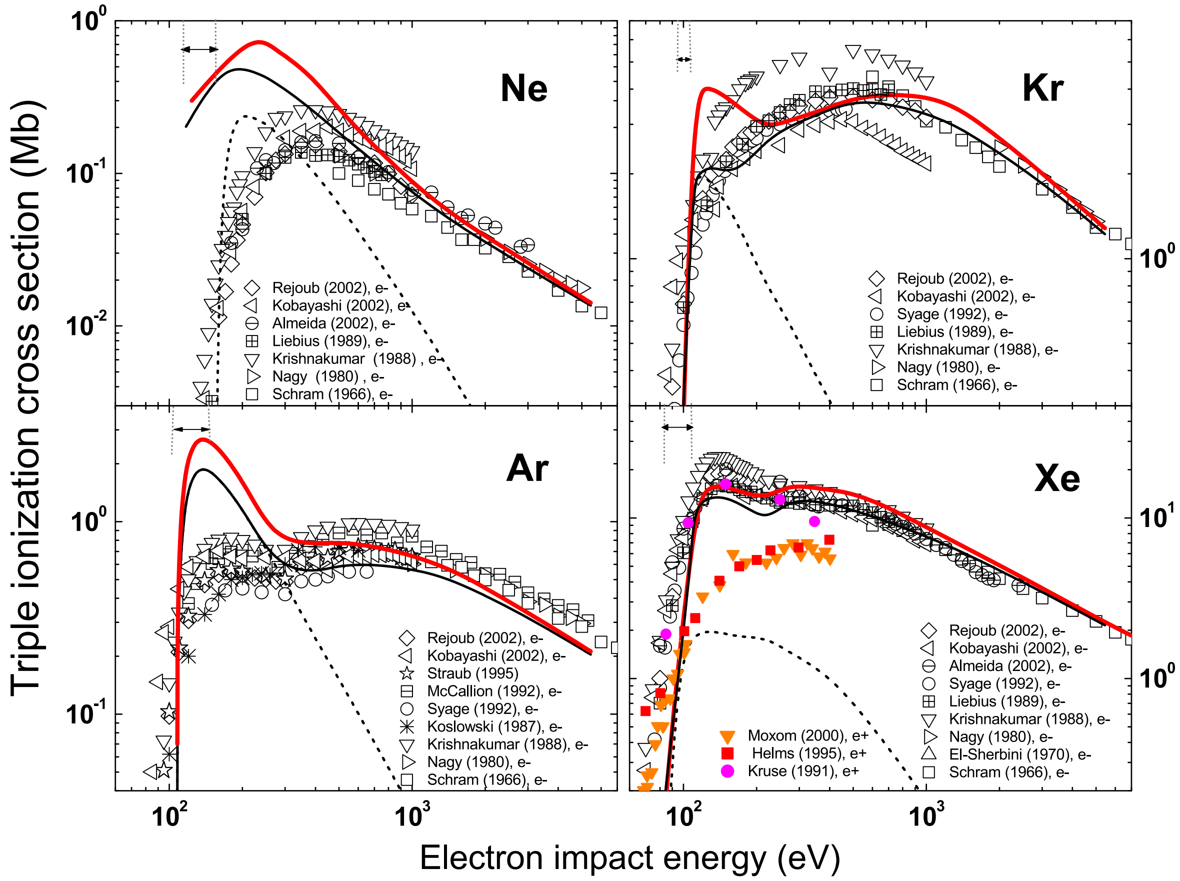

Figure 3. Triple-ionization cross sections of Ne, Ar, Kr and Xe by positron and electron impact. Curves: as in figure 1. Symbols: **for positron impact**, ▼ Moxom [31], ■ Helms *et al* [32] as derived in [31], ● Kruse *et al* [33] as derived in [31]; **for electron impact**, as in figure 2, plus ⋇ Koslowski *et al* [68] for Ar.

4. Results and discussion

4.1. Multiple ionization cross sections

In figures 1–6 we display our positron and electron-impact MI cross sections of Ne, Ar, Kr and Xe, from single to sextuple. For positrons these are the first systematic calculations in such an extended energy range. We compare them with new electron-impact values, calculated as in [36] but considering the threshold energy as described in the previous section. The improvement of the near threshold values is clear. In the figures we have marked with a vertical line the last not-null calculated value. The curves are interpolated from this value to zero cross section at the appearance energy, also marked with a vertical line.

In figure 1 our single-ionization results are shown together with the available experimental data for positron and electron impact. We found that both projectiles have similar behaviour, with the positron values above the electron ones near the maximum. This has been noted by other authors [4] and can be observed in figure 1 in the data by Knudsen *et al* [17] for Ne and Ar, Jacobsen *et al* [18] for Ne or by Kara *et al* [27] for Xe. But it is fair to mention that near the threshold there are positron experimental values equal to and also below the electron ones.

For Ne at high energies our results describe well the electron-impact experimental data by Krishnakumar *et al* [53], Rejoub *et al* [62] and Kobayashi *et al* [63]. These values are above the measurements of Schram [55] and Nagy *et al* [56] at 1 keV. This is important because these are the different values employed in the normalization of the positron data, as mentioned in the previous section.

For Ar in figure 1, the different electron-impact data are quite close to each other and so are our high energy values. For positron impact our theoretical results describe the single ionization measurements above 100 eV. Below this impact energy our cross sections are closer to the values measured by Knudsen *et al* [17] than to the recent data by Jacobsen *et al* [18] and Laricchia *et al* [20]. These measurements show a maximum of the cross sections around 100 eV while Knudsen *et al* [17] and our own results display a maximum at 60 eV. The near-threshold region is always complicated for our theoretical model due to the limitations of the CDW-EIS and the IPM. Experimentally it is a critical region too due to the positronium-formation contribution.

For Kr and Xe, the agreement with the positron data above 80 eV is good. At high energies, the Kr and Xe single-ionization cross sections including PCI are below the single DI, denoted with dotted-curves. This is because part of the single ionization ends up as higher MI.

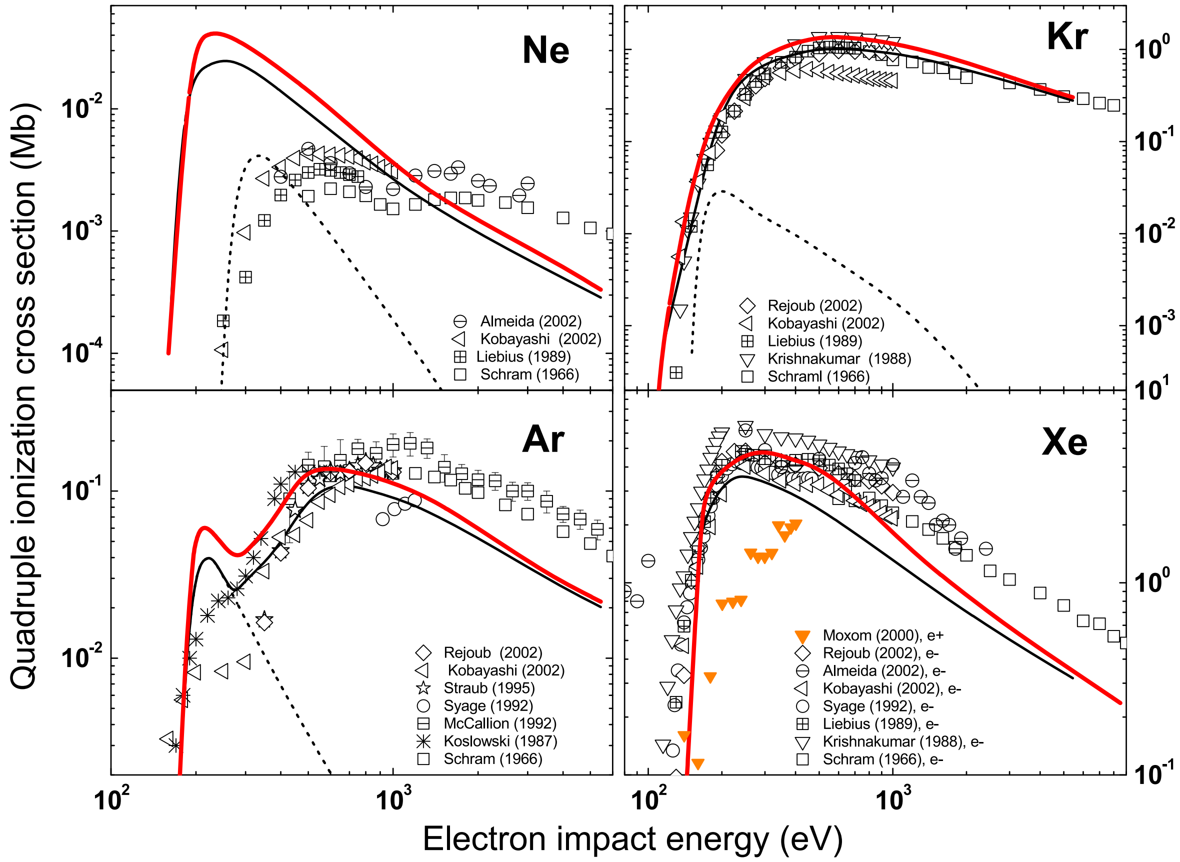

Figure 4. Quadruple-ionization cross sections of Ne, Ar, Kr and Xe by positron and electron impact. Curves as in figure 1. Symbols, experimental data: **for positron impact**, ▼ Moxom [31]; **for electron impact**: □ Schram *et al* [55], ▽ Krishnakumar *et al* [53], ○ Syage [49], ◊ Rejoub *et al* [62], ⊟ McCallion *et al* [64], ◁ Kobayashi *et al* [63], hollow ★ Straub *et al* [65], ⊖ Almeida *et al* [66], ⊞ Liebius *et al* [67], ⋇ Koslowski *et al* [68].

Figure 2 shows our double-ionization results. The solid lines are the ionization cross sections adding DI and PCI and the dotted lines are DI by electron impact. At high energies the positron-impact DI is similar to the electron-impact one. The PCI contribution has been explicitly marked in this figure.

Our positron-impact results are always above the electron-impact ones at intermediate energies (around the maximum of the cross sections) and tend to similar values at high energies. On the other hand, the experimental data for positron impact by Kara *et al* [27] and by Charlton *et al* [26] are below the electron data, even at rather high impact energies. The overall tendency at high energies is correct. We have tested this with the proton-and antiproton-impact double-ionization cross sections (experiments and theory) [35, 36], which clearly converge at high energies. For Ar, Kr and Xe an overestimation of the experimental data can be noted in the above threshold region, but goes down drastically due to the minimum energy given by equation (2). This overestimation is a characteristic of the present model for light particles.

The case of Ne deserves a separate comment. Only for Ne have we included PCI considering the valence shell contribution too, not due to Auger processes, which are energetically not allowed, but due to the change in the Ne binding potential [34, 35]. This gives very good results at high energies but increases in excess in the intermediate energy values, and does not reproduce the threshold at all, although the minimum energy of the equation (2) has been included. No matter the projectile, our attempts to describe the MI of Neon at intermediate to low energies have always failed. Perhaps a different physics is involved (see comments in [39]). A study of multiple ionization of Ne by heavy charged particles has been recently published by Schenk *et al* [69]. This work improves on our previous results in [40] by including charge-exchange processes and projectile electron loss.

The triple-ionization cross sections are displayed in figure 3. To our knowledge, no positron-impact data is available, except for the Xe target: the measurements by Moxom [31], Helms *et al* [32] and Kruse *et al* [33]. The values by Moxom [31] and Helms *et al* [32] are clearly below the electron-impact ones, even for rather high energies (400 eV). Instead the data by Kruse *et al* [33] are in very nice agreement with the electron-impact ones and with our predictions.

Figure 3 shows the good agreement obtained at high energies where the PCI dominates. On the other hand, the thresholds are fairly well described. A two-maximum shape can be noted in the electron-impact experimental values for Ar, Kr and Xe at the impact energy where PCI becomes more

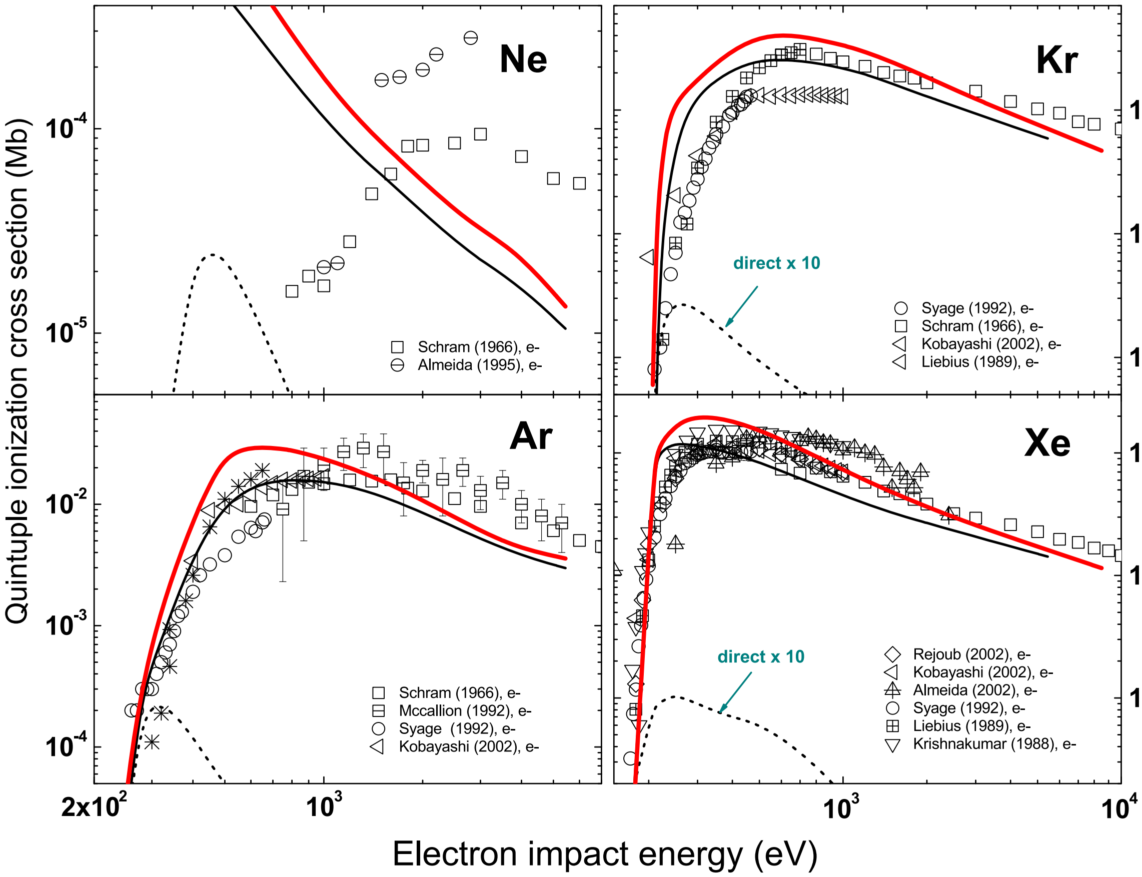

Figure 5. Quintuple-ionization cross sections of Ne, Ar, Kr and Xe by positron and electron impact. Curves as in figure 1. Experimental data **for electron impact**: □ Schram *et al* [55], ▿ Krishnakumar *et al* [53], ∘ Syage [49], ◊ Rejoub *et al* [62], ⊟ McCallion *et al* [64], ◁ Kobayashi *et al* [63], ⊖ Almeida *et al* [66], ⊞ Liebius *et al* [67], ⋇ Koslowski *et al* [68].

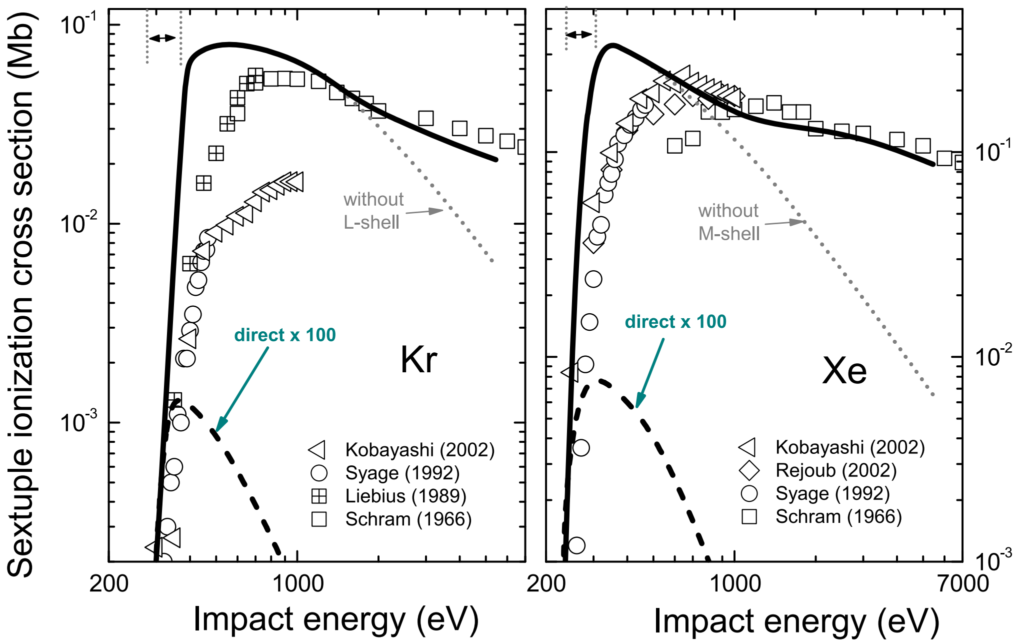

Figure 6. Sextuple-ionization cross sections of Kr and Xe by electron impact. Curves: solid line presents results including direct and post-collisional ionization; dashed line; present results considering only direct ionization. Experimental data: □ Schram *et al* [55],∘ Syage [49], ◊ Rejoub *et al* [62], ◁ Kobayashi *et al* [63], ⊞ Liebius *et al* [67].

important than DI. This two-peak shape is also found in our theoretical curves at the same energies, but is somewhat exaggerated. The tendency to overestimate at intermediate energies has already been found in MI by ion-impact. The IPM (multinomial analysis of the single particle transitions) is one of the limiting factors [39, 70]. Kirchner and collaborators found that DI can be described by an IPM when the final target charge state does not exceed that of the projectile by much more than one [69, 71, 72]. This is valid for ion-impact MI of intermediate targets, such as Ne or Ar. For Kr and Xe the statistical description of the MI given by a multinomial expansion is expected to work better [35]. For electron impact we have found a similar behavior: a clear overestimation of the triple-ionization cross sections for Ar in the energy region where DI dominates (short dashed lines in figure 3); and a rather good description of the triple ionization for Kr and Xe. However, there is an important difference in MI by light-particles. The drastic decrease in the cross sections when approaching from intermediate energies to the threshold makes PCI dominate almost in the whole energy range (see for example Xe in figure 3), and extends the validity of the IPM to higher final target charge states.

The quadruple-ionization cross sections are displayed in figure 4. The description is reasonable for Ar, Kr and Xe. It can be noted that calculations without PCI are two or more orders of magnitude below the data. Moreover, the values for just direct quadruple ionization of Xe are out of scale in figure 4. As usual, our calculations predict positron cross sections slightly above electron ones. On the other hand, the data from Moxom *et al* [31] for positron impact on Xe is below the electron-impact data. It would be interesting to have new measurements, not only for Xe but for the other targets too.

In figure 5 we display our quintuple-ionization cross sections and compare them only with electron-impact data. To our knowledge no measurements have been published for quintuple ionization by positron impact in these targets. Nevertheless we include the theoretical predictions for both electrons and positrons. Our electron-impact cross sections clearly improve on previous ones [36] in the near-threshold region. Quintuple DI is almost negligible even at low energies. To make them visible we have to multiply DI per 10 in the Kr and Xe plots. We stress that for Kr and Xe, deep sub-shells such as Kr-2p and Xe-3d are very important to the PCI [48] and have been included. Again, we can note the chronic disability of the present model to deal with Ne. Instead, this figure shows that Ar, Kr and Xe measurements are very nicely described. For these targets, the quintuple ionization is due to PCI even near the threshold. This is mainly single or double ionization ending in quintuple. As a consequence, the mentioned limitations of the IPM to deal with MI are avoided, and a good description of the inner-shell ionization is highlighted.

Figure 6 shows our total sextuple-ionization values only for electron impact in Kr and Xe. The contributions of the deepest shells are explicitly shown. We have recalculated the values in [36] considering the new energy threshold. Sextuple DI ionization is so small that to fit the scale of this figure we needed to multiply them by 100. Our energy threshold describes rather well the experimental one. Close to this threshold our model overestimates but describes the qualitative trend of the measurements. The agreement with the experimental data is actually very good at high energies, as already noted in [36].

4.2. Total ionization cross sections

Finally, in figure 7 we display the present results for the total (*gross*) ionization cross sections of the four rare gases studied here. As can be noted, the thresholds for each target are well described (see table 1, first column). We have marked with a vertical line the last calculated value. The curves are interpolated from this value to zero cross section for the appearance energy.

The positron-impact data included in figure 7 are total (*gross*) cross sections [19, 21, 27] and single-ionization cross sections [17, 18, 59]. The total values by Kara *et al* [27] for Kr and Xe have been calculated from the MI measurements in [27] as single plus twice double. By doing this, Kara *et al* [27] total cross sections agree quite well with those of Marler *et al* [21].

It can be noted that, at intermediate energies, there are positron measurements above the electron data: Knudsen and collaborators in [17, 18] for Ne and Ar, Mori and Sueoka [19] for Ar, Marler *et al* [21] and Kara *et al* [27] for Xe. But there are also measurements quite close to the electron data, mainly for Ar and Kr.

The positron–electron normalization is crucial, even when it is performed considering the keV values where they are actually the same. We only include in figure 7 the experimental data normalized to *gross* cross sections, not to *count* ones, except for Ne and Ar because the *gross–count* difference is minor in these targets [35]. For example, in the very recent review by Chiari and Zecca [8] the authors noted a discrepancy between the data by Marler [21] and by van Reeth *et al* [59] (see figure 16 in [8]). This is because count cross sections are compared with gross cross sections.

Our CDW-EIS total ionization cross sections by electron and positron impact converge in the high-energy region, as expected. In this region the experiments are nicely described. For lower energies, the electron-impact values agree with the measurements for Kr and Xe and overestimates 20–30% for Ne and Ar. For positron-impact ionization of Ne and Ar, near the maximum our values describe only one set of experimental data, by Knudsen *et al* [17]. For Kr, the positron-impact measurements by Kara *et al* [27] and Marler *et al* [21] are similar to the electron-impact data. We agree with the electron data but clearly overestimate the positron data below 100 eV. For Xe, the description is good in the whole energy range.

This tendency to overestimate the positron-impact data has already been noted in the MI cross sections. Different reasons converge. On one hand are the limitations of the CDW-EIS approximation for low-energy light particles (see comments in [36]). On the other hand, positron scattering at low energies will be affected by positronium formation. Even within the IPM, the inclusion of a two-center description

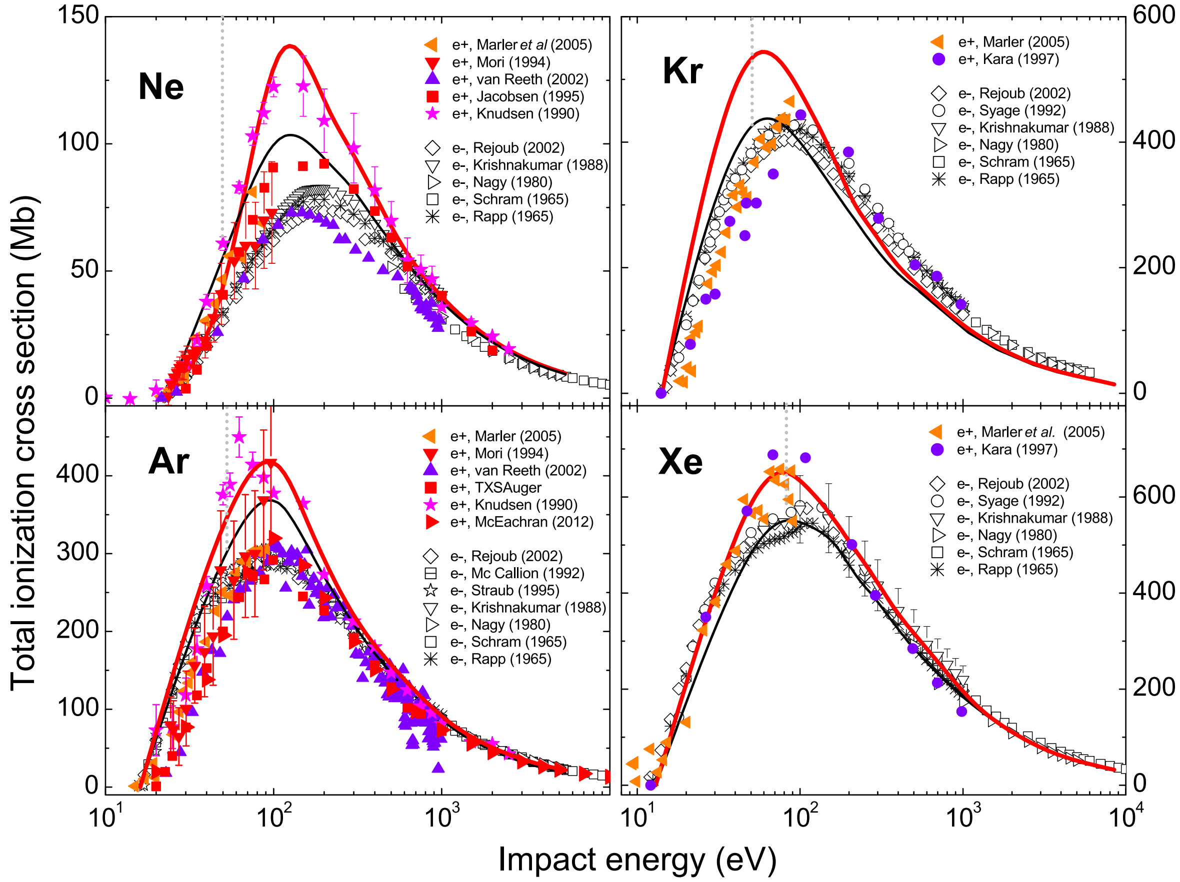

Figure 7. Total ionization cross section of Ne, Ar, Kr and Xe by positron and electron impact. Curves present results for total ionization cross sections including PCI by positron impact (thick redline) and by electron impact (thin blackline). Experimental data: **total ionization by positron impact**, ◀ by Marler *et al* [21], ▾ by Mori and Sueoka [19], ● Kara *et al* [27] (single plus 2 × double), ▶ by McEachran *et al* [10] (suggested values for positron-Ar); **single ionization by positron impact**, ▲ van Reeth *et al* [59], ■ Jacobsen *et al* [18], ☆ Knudsen *et al* [17]; **total ionization by electron impact**, □ Schram *et al* [55], ⋇ Rapp and Eglander-Golden [54], ▷ Nagy *et al* [56], ▿ Krishnakumar *et al* [53], ◊ Rejoub *et al* [62]. The vertical dotted grey line indicates the last not-null value calculated. We interpolate between this value and zero at the appearance energy.

considering capture and ionization may improve these results [69]. The importance of the positronium formation in the range of energies included in figure 7 depends on the target. Following Laricchia *et al* [20] and Marler *et al* [21], the positronium formation cross section for Ne has a maximum around 30 eV and is still important at 100 eV. This shifts to lower energies for a heavier target, with the maximum for Xe being around 10 eV and almost negligible above 70 eV [15, 21].

Our total ionization cross sections by positrons are always above the electron-impact ones, and both converge around 600 keV for Ne and Ar, and 1 keV for Kr and Xe. Instead, we have found that the positron-impact cross sections converge to the equal-velocity proton-impact ones [36] at even lower energies (300 eV for Ne and Ar, 600 eV for Kr and Xe): equal charge seems to be more decisive than equal mass.

Recently, McEachran *et al* [10] derived and tabulated recommended positron-Ar cross sections based on the experimental data available and theoretical considerations. Our *ab initio* values are in general above those of McEachran *et al* [10], except in the keV region.

It is important to stress that if PCI is not taken into account the total ionization cross sections for Kr and Xe in the keV region are 20–30% below the experimental data by Schram [55] or Nagy *et al* [56] as noted in [35, 36]. A similar difference is found between the total cross sections and the *count* cross sections [35].

We did not include in figure 7 other theoretical results for positron-impact ionization cross sections such as those found in [22–25]. A compilation of them is presented in the review by Chiari and Zecca [8]. Our theoretical results are in agreement with the calculations by Moores [24] and Bartschat [22] for Ar and Xe (the latter only around the maximum, not for low energies).

5. Conclusions

In this work we have presented positron-impact multiple as well as total ionization cross sections of Ne, Ar, Kr, and Xe covering an extended energy range. The theoretical model employed is the CDW-EIS for light particles, following the same scheme of our previous work [36]. We have obtained good results even for quadruple-, quintuple- and sextuple-ionization cross sections. This is related to the good description of the deep-shell contribution and the post-collisional ionization. We have found that for highly charged ion production by light particles the post-collisional ionization is the main ionization channel in the whole energy range. A novel contribution of the present work is the correction of the energy threshold for the *k*-fold ionization events by including the mean kinetic energy transferred to the emitted electrons. We have employed this energy threshold for positron and electron-impact multiple ionization at the deepest of the multinomial distribution. In this way we highly improved previous electron-impact results in the threshold region. We have also presented particle–antiparticle comparison by including the large amount of data available in the literature. We expect that the present theoretical results may be a motivation for future positron-impact measurements.

Acknowledgments

This work was supported by the following institution of Argentina: Consejo Nacional de Investigaciones Científicas y Técnicas (CONICET), Agencia Nacional de Promoción Científica y Tecnológica, and Universidad de Buenos Aires (UBA).

References

[1] McGuire J H 1986 *Positron (Electron)-Gas Scattering* ed W E Kauppila, T S Stein and J M Wadehra (Singapore: World Scientific) 222–31
[2] Schultz D R, Olson R E and Reinhold C 1991 *J. Phys. B: At. Mol. Opt. Phys.* **24** 521–58
[3] Knudsen H and Reading J F 1992 *Phys. Rep.* **212** 107–222
[4] Paludan K *et al* 1997 *J. Phys. B: At. Mol. Opt. Phys.* **30** 581–7
[5] Charlton M and Humberston J W 2001 *Positron Physics* (Cambridge: Cambridge University Press)
[6] Laricchia G, Armitage S, Köver A and Murtagh D J 2008 *Adv. At. Mol. Opt. Phys.* **56** 1–47
[7] Laricchia G, Cooke D A, Köver A and Brawley S J 2013 *Fragmentation Processes Topics in Atomic and Molecular Physics* ed C T Whelan vol 56 (Cambridge: Cambridge University Press) pp 116–36 (Experimental Aspects of Ionization Studies by Positron and Positronium Impact)
[8] Chiari L and Zecca A 2014 *Eur. Phys. J.* D **68** 297
[9] Kövér Á, Williams A I, Murtagh D J, Fayer S E and Laricchia G 2014 *Meas. Sci. Technol.* **25** 075013
[10] McEachran R P *et al* 2012 *J. Phys. B: At. Mol. Opt. Phys.* **45** 045207
[11] Jacobsen F M, Frandsen N P, Knudsen H and Mikkelsen U 1995 *J. Phys. B: At. Mol. Opt. Phys.* **28** 4675–89
[12] Arcidiacono C, Kövér A and Laricchia G 2005 *Phys. Rev. Lett.* **95** 223202
[13] DuBois R D 2012 *New J. Phys.* **14** 025004
[14] DuBois R D 2014 *J. Phys. Conf. Ser* **488** 012054
[15] Cooke D A, Murtagh D J and Laricchia G 2010 *Phys. Rev. Lett.* **104** 073201
[16] Cooke D A, Murtagh D J and Laricchia G 2014 *Eur. Phys. J.* D **68** 66
[17] Knudsen H, Brun-Nielsen L, Charlton M and Poulsen M R 1990 *J. Phys. B: At. Mol. Opt. Phys.* **23** 3955–76
[18] Jacobsen F M, Frandsen N P, Knudsen H, Mikkelsen U and Schrader D M 1995 *J. Phys. B: At. Mol. Opt. Phys.* **28** 4691–5
[19] Mori S and Sueoka O 1994 *J. Phys. B: At. Mol. Opt. Phys.* **27** 4349–64
[20] Laricchia G, van Reeth P, Szuinska M and Moxom J 2002 *J. Phys. B: At. Mol. Opt. Phys.* **35** 2525–40
[21] Marler J P, Sullivan J P and Surko C M 2005 *Phys. Rev.* A **71** 022701
[22] Bartschat K 2005 *Phys. Rev.* A **71** 032718
[23] Campeanu R I, McEachran R P and Stauffer A D 2002 *Nucl. Instrum. Methods Phys. Res.* B **192** 2002
[24] Moores D L 1998 *Nucl. Instrum. Methods Phys. Res.* B **143** 105
[25] McEachran R P and Stauffer A D 2010 *J. Phys. B: At. Mol. Opt. Phys.* **43** 215209
[26] Charltoni M, Brun-Nielsen L, Deutch B I, Hvelplund P, Jacobsen F M, Knudsen H, Laricchiat G and Poulsen M R 1989 *J. Phys. B: At. Mol. Opt. Phys.* **22** 2779–88
[27] Kara V, Paludan K, Moxom J, Ashley P and Laricchia G 1997 *J. Phys. B: At. Mol. Opt. Phys.* **30** 3933–49
[28] Moxom J, Ashley P and Laricchia G 1996 *Can. J. Phys.* **74** 367
[29] Moxom J, Schrader D M, Laricchia G, Xu J and Hulett1 L D 1999 *Phys. Rev.* A **60** 2940–3
[30] Bluhme H, Knudsen H, Merrison J P and Nielsen K A 1999 *J. Phys. B: At. Mol. Opt. Phys.* **32** 5237
[31] Moxom J 2000 *J. Phys. B: At. Mol. Opt. Phys.* **33** 481–5
[32] Helms S, Brinkmann U, Deiwiks J, Hippler R, Schneider H, Segers D and Paridaens J 1995 *J. Phys. B: At. Mol. Opt. Phys.* **28** 1095
[33] Kruse G, Quermann A, Raith W, Sinapius G and Weber M 1991 *J. Phys. B: At. Mol. Opt. Phys.* **24** L33
[34] Montanari C C, Montenegro E C and Miraglia J E 2010 *J. Phys. B: At. Mol. Opt. Phys.* **43** 165201
[35] Montanari C C and Miraglia J E 2012 *J. Phys. B: At. Mol. Opt. Phys.* **45** 105201
[36] Montanari C C and Miraglia J E 2014 *J. Phys. B: At. Mol. Opt. Phys.* **47** 105203
[37] Cavalcanti E G, Sigaud G M, Montenegro E C, Sant 'Anna M M and Schmidt-Bocking H 2002 *J. Phys. B: At. Mol. Opt. Phys.* **35** 3937
[38] Spranger T and Kirchner T 2004 *J. Phys. B: At. Mol. Opt. Phys.* **37** 4159
[39] Montanari C C, Miraglia J E, Wolff W, Luna H, Santos A C F and Montenegro E C 2012 *J. Phys. Conf. Series* **388** 012036
[40] Wolff W *et al* 2011 *Phys. Rev.* A **84** 042704
[41] Montanari C C and Miraglia J E 2015 *J. Phys. Conf. Series* **583** 012018
[42] Gstir B *et al* 2002 *J. Phys. B: At. Mol. Opt. Phys.* **35** 2993
[43] Denifl S *et al* 2002 *J. Phys. B: At. Mol. Opt. Phys.* **35** 4685
[44] Wannier G H 1955 *Phys. Rev.* **100** 1180
[45] Ashley P, Moxom J and Laricchia G 1996 *Phys. Rev. Lett.* **77** 1250
[46] van Reeth P, Humberston J W and Laricchia G 2001 *J. Phys. B: At. Mol. Opt. Phys.* **34** 271–9
[47] McDowell M R C and Coleman J P 1970 *Introduction to the Theory of Ion-Atom Collisions* (Amsterdam: North-Holland) ch 3
[48] Tavares A C, Montanari C C, Miraglia J E and Sigaud G M 2014 *J. Phys. B: At. Mol. Opt. Phys.* **47** 045201
[49] Syage J A 1992 *Phys. Rev.* A **46** 5666
[50] Carlson T A, Hunt W E and Krause M O 1966 *Phys. Rev.* **151** 41
[51] Carlson T A and Krause M O 1965 *Phys. Rev. Lett.* **14** 390
[52] Galassi M E, Rivarola R D and Fainstein P D 2007 *Phys. Rev.* A **75** 052708
[53] Krishnakumar E and Srivastava S K 1988 *J. Phys. B: At. Mol. Opt. Phys.* **21** 1055–82

[54] Rapp D and Englander-Golden P 1965 *J. Chem. Phys.* **43** 1464
[55] Schram B L, Boerboom A J H and Kistermaker J 1966 *Physica* **32** 185–96
Schram B L 1966 *Physica* **32** 197–209
Schram B L, de Heer F J, van der Wiel M J and Kistermaker J 1965 *Physica* **31** 94
Adamczyk B, Boerboom A J H, Schram B L and Kistermaker J 1966 *J. Chem. Phys.* **44** 4640–2
[56] Nagy P, Skutlartz A and Schmidt V 1980 *J. Phys. B: At. Mol. Opt. Phys.* **13** 1249–67
[57] Sorokin A A, Shmaenok L A, Bobashev S V, Möbus B, Richter M and Ulm G 2000 *Phys. Rev* A **61** 022723
[58] Sorokin A A, Shmaenok L A, Bobashev S V, Möbus B and Ulm G 1998 *Phys. Rev.* A **58** 2900
[59] van Reeth P, Szluinska M and Laricchia G 2002 *Nucl. Instrum. Methods Phys. Res.* B **192** 220
[60] Sant'Anna M M, Montenegro E C and McGuire J H 1998 *Phys. Rev.* A **58** 2148–59
[61] de Heer F J, Jansen R H J and van der Kaay W 1979 *J. Phys. B: At. Mol. Opt. Phys.* **12** 979–1002
[62] Rejoub R, Lindsay B G and Stebbing R F 2002 *Phys. Rev.* A **65** 042713
[63] Kobayashi A, Fujiki G, Okaji A and Masuoka T 2002 *J. Phys. B: At. Mol. Opt. Phys.* **35** 2087–103
[64] McCallion P, Shah M B and Gilbody H B 1992 *J. Phys. B: At. Mol. Opt. Phys.* **25** 1061–71
[65] Straub H C, Renault P, Lindsay B G, Smith K A and Stebbings R F 1995 *Phys. Rev.* A **52** 1115–24
[66] Almeida D P, Fontes A C and Godinho C F L 1995 *J. Phys. B: At. Mol. Opt. Phys.* **28** 3335–45
[67] Liebius H, Binder J, Koslowwski H R, Wiesemann K and Huber B A 1989 *J. Phys. B: At. Mol. Opt. Phys.* **22** 83–97
[68] Koslowski H R, Binder J, Huber B A and Wiesemann K 1987 *J. Phys. B: At. Mol. Opt. Phys.* **20** 5903
[69] Schenk G, Horbatsch M and Kirchner T 2013 *Phys. Rev.* A **88** 012712
[70] Kirchner T, Lüdde H J and Dreizler R M 1999 *Phys. Rev.* A **61** 012705
[71] Kirchner T, Horbatsch M, Lüdde H J and Dreizler R M 2000 *Phys. Rev.* A **62** 042704
[72] Kirchner T, Horbatsch M and Lüdde H J 2001 *Phys. Rev.* A **64** 012711
Kirchner T, Horbatsch M and Lüdde H J 2002 *Phys. Rev.* A **66** 052719